the FEBS Journal

The specificity and kinetic mechanism of branched-chain amino acid aminotransferase from *Escherichia coli* studied with a new improved coupled assay procedure and the enzyme's potential for biocatalysis

Xuejing Yu[1], Xingguo Wang[2] and Paul C. Engel[1]

1 School of Biomolecular and Biomedical Science, Conway Institute, University College Dublin, Ireland
2 Faculty of Life Science, Hubei University, Wuhan, China

Keywords
branched-chain amino acid amino-transferase; kinetic mechanism; non-natural amino acids; rate-limiting step; substrate specificity

Correspondence
P. C. Engel, School of Biomolecular and Biomedical Science, Conway Institute, University College Dublin, Belfield, Dublin 4, Ireland
Fax: +353 1 283 7211
Tel: +353 1 716 6764
E-mail: paul.engel@ucd.ie

(Received 9 August 2013, revised 3 November 2013, accepted 7 November 2013)

doi:10.1111/febs.12609

Branched-chain amino acid aminotransferase (BCAT) plays a key role in the biosynthesis of hydrophobic amino acids (such as leucine, isoleucine and valine), and its substrate spectrum has not been fully explored or exploited owing to the inescapable restrictions of previous assays, which were mainly based on following the formation/consumption of the specific branched-chain substrates rather than the common amino group donor/acceptor. In our study, detailed measurements were made using a novel coupled assay, employing (*R*)-hydroxyglutarate dehydrogenase from *Acidaminococcus fermentans* as an auxiliary enzyme, to provide accurate and reliable kinetic constants. We show that *Escherichia coli* BCAT can be used for asymmetric synthesis of a range of non-natural amino acids such as L-norleucine, L-norvaline and L-neopentylglycine and compare the kinetic results with the results of molecular modelling. A full two-substrate steady-state kinetic study for several substrates yields results consistent with a bi-bi ping-pong mechanism, and detailed analysis of the kinetic constants indicates that, for good 2-oxoacid substrates, release of 2-oxoglutarate is much slower than release of the product amino acid during the transamination reaction. The latter is in fact rate-limiting under conditions of substrate saturation.

Database
Branched-chain amino acid aminotransferase EC 2.6.1.42; (*R*)-2-hydroxyglutarate dehydrogenase EC 1.1.99.2

Introduction

The metabolism of amino acids typically involves a two-stage interconversion between inorganic nitrogen, as ammonia, and amino group nitrogen. Glutamate, and sometimes alanine or glutamine, serve as the entry or exit points for ammonia, utilizing a small number of oxidoreductases of narrow specificity such as glutamate dehydrogenase, alanine dehydrogenase and glutamate synthase. The funnelling through these few enzymes relies on interfacing with a set of aminotransferases of wider specificity, which distribute amino groups to, or gather amino groups from, a range of different carbon skeletons. Apart from their evident metabolic importance, aminotransferases have biotechnological potential in view of their ability to handle a considerable

Abbreviations
BCAT, branched-chain amino acid aminotransferase; GDH, L-glutamate dehydrogenase; HGDH, (*R*) -2-hydroxyglutarate dehydrogenase; PLP, pyridoxal 5′-phosphate.

range of substrates. In practice, they have been increasingly applied to large-scale synthesis of non-natural amino acids, which can be used as the building blocks for peptidomimetic and other single-enantiomer drugs in the pharmaceutical industry [1–4]. The most widely investigated are the α-transaminases, e.g. aspartate aminotransferase, tyrosine aminotransferase, valine-pyruvate aminotransferase and branched-chain amino acid aminotransferase of *Escherichia coli* K-12 [5]. These enzymes catalyse reversible pyridoxal 5′-phosphate (PLP) dependent transfer of an amino group to a 2-oxoacid acceptor from a donor, most frequently L-glutamate, yielding a new amino acid and the 2-oxoacid product corresponding to the donor (2-oxoglutarate in the case of L-glutamate). Aminotransferases have several advantages over other biocatalysts, including high reaction rates and enantioselectivity and the low cost of the amino donor, glutamate. Also, since the PLP is a tightly bound prosthetic group there is no requirement for bulk addition or recycling of a cofactor, as with amino acid dehydrogenases. However, this last, practically attractive feature of aminotransferase biocatalysis carries a penalty, as the overall reaction offers no convenient spectrophotometric change to serve as the basis of a continuous assay. Inevitably this complicates studies of kinetics and in particular of substrate specificity. We have recently addressed this problem by introducing a novel coupled assay [6] using a bacterial (*R*)-2-hydroxyglutarate dehydrogenase (HGDH) as an auxiliary enzyme (Fig. 1). Oxoglutarate generated in the transamination reaction is continuously reduced by NADH, and thus the decrease in A_{340} can be used to monitor the reaction. Crucially, since the coupling reaction involves the glutamate/oxoglutarate couple rather than the other variable substrate pair, the assay not only can be applied to many aminotransferases but also for any given one can be used reliably for comparative

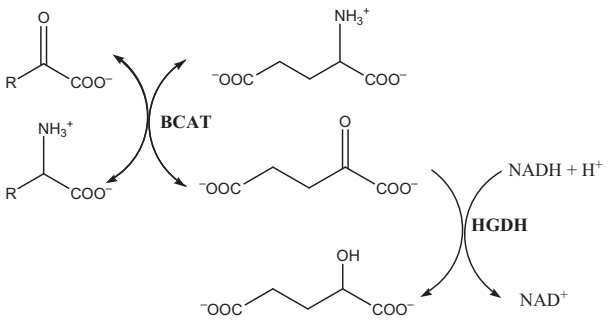

Fig. 1. Coupled assay system to measure BCAT activity. The assay procedure is based on NADH depletion in the HGDH reaction. R is for example isopropyl, isobutyl or 2-methylbutyl [6].

assays to assess substrate specificity and also possible changes in specificity through mutagenesis. The availability of a convenient and reliable continuous assay has opened the door to ready kinetic analysis and to thorough quantitative studies of mechanism and specificity.

In our study, the branched-chain amino acid aminotransferase BCAT (EC 2.6.1.42) was used as a starting point to explore the substrate range in order to assess this enzyme's full potential capacity for producing non-natural amino acids. Classified as transaminase B in 1979 [7], *E. coli* BCAT was initially characterized by coupled assays employing glutamate dehydrogenase (GDH) as auxiliary enzyme. However, significant product inhibition of GDH was observed at low glutamate concentration and this is inescapable since glutamate serves as both substrate for BCAT and product for GDH [6]. Further characterization was carried out in 1988 by Inoue *et al.* [8], who determined detailed kinetic parameters in the direction of glutamate formation by the method of Velick and Vavra [9], but only for biological amino acids. They reported that *E. coli* BCAT shows activity towards various aliphatic amino acids, of which L-isoleucine was the best substrate, showing the highest catalytic efficiency value (k_{cat}/K_m). There is a need to obtain similarly accurate kinetic parameters of BCAT in the opposite direction of reaction and for a wider range of branched-chain 2-oxoacids, including those corresponding to non-natural amino acids of industrial interest. Such information would be of importance for evaluating process technology options [10]. Earlier studies [11–15] had alerted us to the potential of BCAT as a biocatalyst for production of high-value non-natural amino acids, such as L-*tert*-leucine and L-3-hydroxyadamantylglycine. Therefore, the overall substrate specificity and kinetic properties of *E. coli* BCAT have been revisited using the novel coupled assay, which delivers reliable initial-rate measurements. In our hands, BCAT showed broad applicability to the synthesis of non-natural aliphatic branched-chain amino acids, such as L-norleucine, L-norvaline, L-*tert*-leucine and L-neopentylglycine, which can be used as building blocks for pharmaceutical drug synthesis [16,17]. The detailed analysis has also yielded new insight into the kinetic features of the reaction which should guide thinking in future protein engineering of this enzyme.

Results

Characterization of BCAT

The recombinant BCAT, purified via a three-step procedure [6], gave a single band on an SDS/PAGE gel

(> 90% purity) with the correct apparent molecular mass (3.5×10^4 Da for the subunit). In all cases, 1.82×10^5 Da, calculated by Lee-Peng *et al.* [7], was used as total protein molecular mass. Under the standard coupled assay conditions, initial velocities were proportional to enzyme concentration in the range 0–0.08 μM (calculated on an oligomer basis). In all cases, 1 unit of enzyme activity is defined as the amount of enzyme required to catalyse the oxidation of 1 μmol NADH per minute in the 100 mM Tris/HCl (pH 8.0) buffer containing 10 mM glutamate and 10 mM 2-oxoisocaproate at 37 °C. The specific activity of purified BCAT in this assay system was 7.7 $U \cdot mg^{-1}$.

Substrate specificity

As described in previous literature [18,19], transaminases are subject to inhibition by substrate and product. In order to avoid substrate inhibition, a low steady-state concentration of L-glutamate (10 mM) was kept throughout the assays to profile substrate specificity. The apparent K_m and k_{cat} values for nine 2-oxoacids as amino acceptor at this fixed concentration of L-glutamate as amino donor are shown in Table 1. Under the conditions applied, 3-methyl-2-oxopentanoate and 2-oxoisocaproate, the oxoacid salts corresponding to L-isoleucine and L-leucine respectively, appeared to be the best branched-chain substrates, with similar apparent K_m values (0.07 mM and 0.08 mM respectively) and similar apparent k_{cat} values. There was also remarkable constancy in the k_{cat} values for all oxoacid substrates with at least a 5-carbon chain, with the exception of 4,4-dimethyl-2-oxopentanoate (product L-neopentylglycine), which is presumably somewhat sterically hindered and gave a value ~ 50% lower. By contrast, the specificity constant k_{cat}/K_m for trimethylpyruvate (product L-*tert*-leucine) is nearly 81-fold smaller than that towards natural substrate 3-methyl-2-oxopentanoate (4.07 $mM^{-1} \cdot s^{-1}$ versus 329 $mM^{-1} \cdot s^{-1}$). Surprisingly, the K_m value of BCAT for 2-oxovalerate (product L-norvaline) was 7.5-fold higher than that for 2-oxoisocaproate (0.6 mM versus 0.08 mM), while k_{cat} values were similar. In the case of pyruvate, it is noteworthy that Inoue *et al.* [8] reported that this oxoacid cannot serve as an amino acceptor for BCAT. In fact, although its K_m is very high (~ 57 mM), the k_{cat} value is only 5-fold lower than that for the best substrates. In view of the demonstrated broad range of substrate specificity for the larger substrates, BCAT shows excellent potential for asymmetric synthesis of several non-natural amino acids, for instance L-norleucine, L-norvaline and L-neopentylglycine.

Molecular modelling of substrate binding in BCAT

In order to investigate the basis of substrate specificity, the three-dimensional structure of the *E. coli* BCAT complex with the substrate analogue 2-methylleucine (2.4 Å resolution) (PDB Accession No. 1I1L) [20,21] was used as a template to model the binding of various natural and non-natural branched-chain amino acids: L-leucine, L-isoleucine, L-norleucine, L-norvaline, L-*tert*-leucine (shown in Fig. 2). All amino acids were modelled to sit in the active site of *E. coli* BCAT in the most energetically favourable conformation. The inner side of the pocket (shown in green and molecular surface form) was demonstrated to bind the hydrophobic side chain and the α-carboxylate group of the substrates. Various side chains of substrates could be accepted because of the wide binding pocket. In the earlier kinetics study, 2-oxoacids corresponding to L-leucine and L-isoleucine (Fig. 2b,c), which gave maximal k_{cat} values combined with the lowest K_m values, were considered as the best substrates of BCAT among the above compounds. This indicates that a methyl group in either the C^{β} position or the C^{γ} position does not impede the binding. L-norleucine, which has a carbon backbone longer by one carbon unit, was a somewhat poorer substrate, displaying a loose connection with Y129 or F36 as shown in Fig. 2d. As for a smaller molecule, such as L-*tert*-leucine, its shorter carbon main chain results in weak interaction with the hydrophobic binding pocket (Fig. 2f).

Validation of a ping-pong mechanism and detailed kinetic analysis

For a more thorough analysis, yielding insight into the kinetic mechanism, it is necessary to carry out a systematic variation of the concentrations of the two substrates. Assuming that the dependence of the initial reaction rate on substrate concentration follows simple Michaelis–Menten behaviour for both substrates, the initial-rate equation can be represented in its simple reciprocal form [22,23]:

$$\frac{e}{v} = \phi_o + \frac{\phi_A}{[A]} + \frac{\phi_B}{[B]} + \frac{\phi_{AB}}{[A][B]} \qquad (1)$$

If A and B are designated as glutamate and 2-oxoacid respectively, then all four constants in Eqn (1) can be obtained by carrying out initial-velocity measurements at varying concentrations of B for a series of fixed concentrations of A. The Lineweaver–Burk plots of e/v against $1/[B]$ should be a series of lines, and slopes and ordinate intercepts are measured for

Table 1. Kinetic parameters of BCAT towards a range of natural and non-natural 2-oxoacids.

Substrate	Corresponding amino acid	Structure	K_m (mM)	k_{cat} (s^{-1})	k_{cat}/K_m ($mM^{-1}·s^{-1}$)
3-Methyl-2-oxopentanoate	L-isoleucine	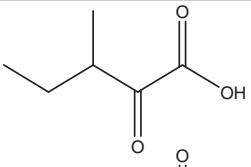	0.07 ± 0.008	23.0 ± 1.2	329
2-Oxoisocaproate	L-leucine	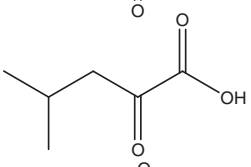	0.08 ± 0.013	24.7 ± 0.87	309
2-Oxoisovalerate	L-valine	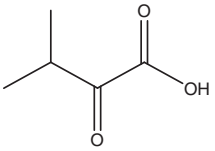	0.20 ± 0.012	10.5 ± 0.11	52.5
2-Oxohexanoate	L-orleucine	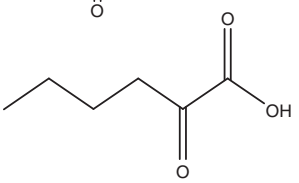	0.22 ± 0.026	23.1 ± 0.34	105
2-Oxovalerate	L-norvaline	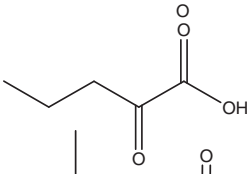	0.60 ± 0.027	25.9 ± 0.72	43.2
4,4-Dimethyl-2-oxopentanoate	L-neopentylglycine	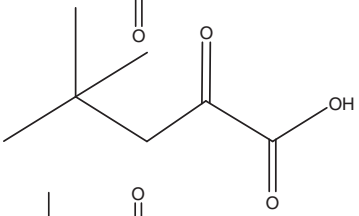	0.08 ± 0.005	12.4 ± 0.12	155
Trimethylpyruvate	L-*tert*-Leucine	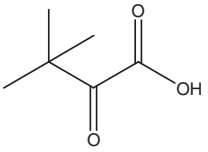	0.15 ± 0.006	0.61 ± 0.05	4.07
Pyruvate	L-alanine	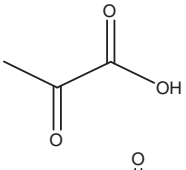	56.8 ± 1.8	4.88 ± 0.17	0.09
2-Oxobutyrate	L-α-Aminobutyric acid	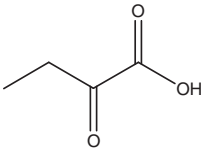	3.37 ± 0.28	13.9 ± 0.61	4.12

Assay mixtures (1 mL) contained 100 mM Tris/HCl (pH 8.0), 0.13 mM NADH, 10 mM glutamate, purified BCAT and coupling enzyme (HGDH) plus 2-oxoacid at concentrations varying from 0.01 mM to 10 mM.

each one. The changing intercepts $\phi_0 + \phi_A/[A]$, reciprocals of the apparent V_{max} for each glutamate concentration, are replotted against 1/[A] in a secondary plot, where the slope is ϕ_A and the ordinate intercept is ϕ_0. The slopes can be similarly replotted to give ϕ_{AB} as the slope and ϕ_B as the intercept. All constants can equally be obtained in different pairs by the alternative graphical procedure of plotting e/v initially

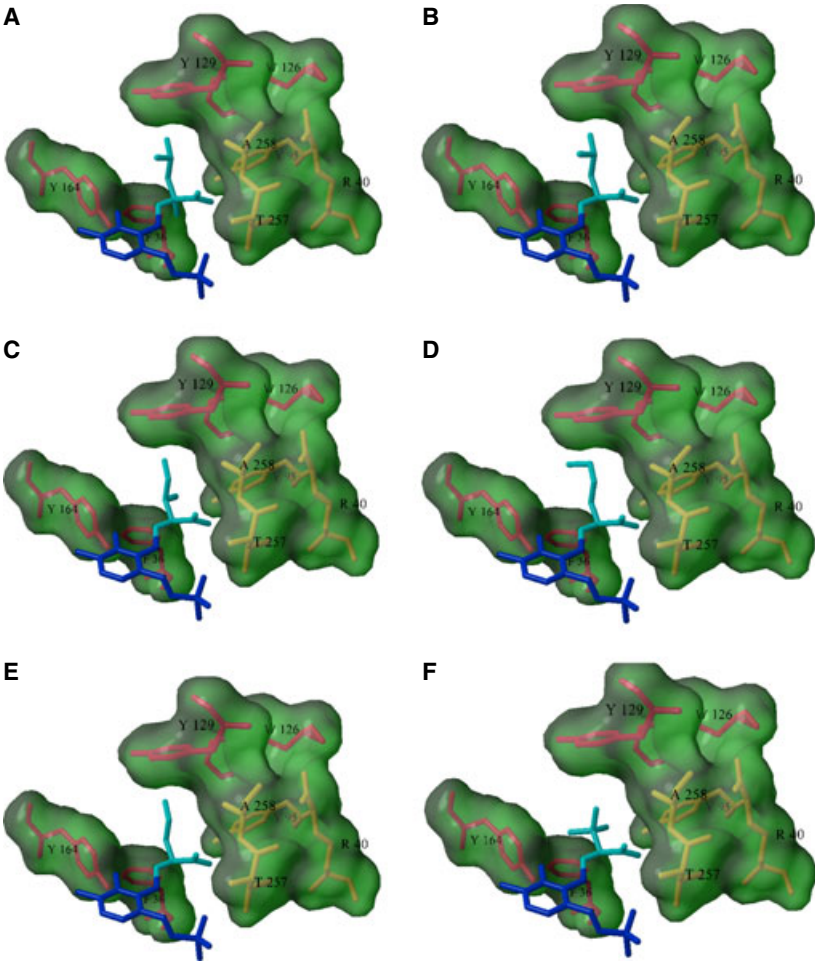

Fig. 2. Models of BCAT bound with various amino acids. The active site region in BCAT (as a molecular surface in green), the protein residues (in red) that make contact with the hydrophobic side chain of the substrates and residues (in yellow) that bind the α-carboxylate group of the substrates are depicted. The cofactor PLP (in dark blue) is shown in the ball and stick form. The various substrates (in light blue) are (A) 2-methylleucine; (B) L-leucine; (C) L-isoleucine; (D) L-norleucine; (E) L-norvaline; (F) L-*tert*-leucine (software YASARA).

against 1/[A] and then replotting slopes and intercepts against 1/[B].

A series of experiments was accordingly performed to measure initial rates of reaction, systematically varying the concentration of 2-oxoisocaproate (0.01–0.5 mM) at each of a series of fixed concentrations of L-glutamate (2–8 mM) in a final volume of 1 mL. Apart from the substrate concentrations, all other conditions were kept constant. An unambiguous parallel-line pattern in the Lineweaver–Burk double reciprocal plots of rate versus 2-oxoisocaproate concentrations at different L-glutamate concentrations (Fig. 3) indicates a ping-pong mechanism, as found for most aminotransferases [9,22,23]. In Fig. 3, where each line is for a different fixed glutamate concentration, ϕ_B emerges as the constant slope of the parallel lines. The constancy of the slope means that in Eqn (1) the ϕ_{AB} term is missing (ϕ_{AB} is zero). The changing intercepts are given by $\phi_0 + \phi_{2\text{-oxoisocaproate}}/[2\text{-oxoisocaproate}]$, so that, in the secondary replot against 1/[2-oxoisocaproate] (Fig. 4A), the slope is $\phi_{2\text{-oxoisocaproate}}$ and the ordinate intercept is ϕ_0. The three constants are given

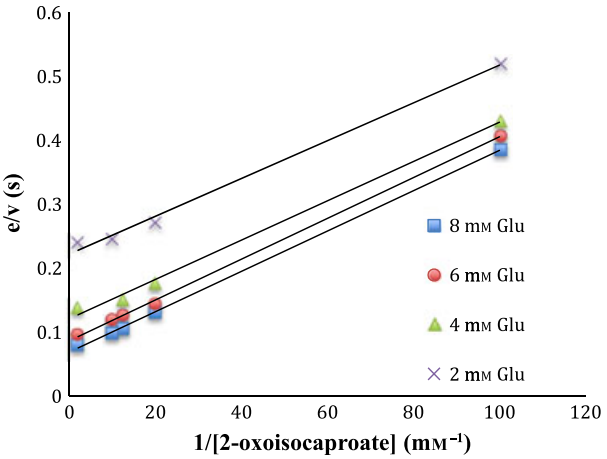

Fig. 3. Double reciprocal plots of reaction rates for variable concentrations of 2-oxoisocaproate at various concentrations of L-glutamate. 2-Oxoisocaproate was varied from 0.01 mM to 0.5 mM as amino acceptor for each of four different concentrations of L-glutamate: 2 mM, 4 mM, 6 mM and 8 mM. The concentration of NADH for the coupling reaction was fixed at 0.13 mM. Reaction velocities were measured from the decrease in absorbance of NADH at 340 nm.

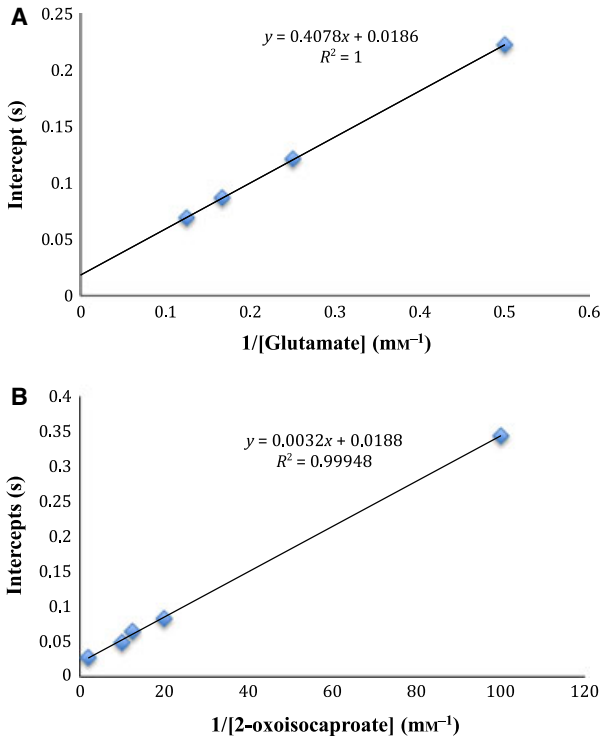

Fig 4. Reaction of 2-oxoisocaproate (B) with L-glutamate (A). (a) Replots of primary intercepts ($\phi_0 + \phi_B/[B]$) against 1/[glutamate]. (b) Replots of primary intercepts ($\phi_0 + \phi_A/[A]$) against 1/[2-oxoisocaproate].

in Table 2. They can equally be obtained by the alternative graphical procedure of plotting e/v initially against 1/[2-oxoisocaproate] and then replotting intercepts against 1/[glutamate] (Fig. 4b). The resulting estimates of the constants are also given in Table 2 and the close agreement between the two estimates of each constant gives a good indication of the reliability of the graphical analysis. From this analysis, the extrapolated k_{cat}, $1/\phi_0$, is 53.5 s^{-1}. The extrapolated Michaelis constants for glutamate and 2-oxoisocaproate, ϕ_A/ϕ_0 and ϕ_B/ϕ_0 respectively, are 21.8 mM and 0.17 mM.

This kinetic pattern, supporting a ping-pong mechanism, in which there is no ternary complex containing both substrates simultaneously, is in full agreement with earlier results both for BCAT and for other aminotransferases [8,9]. The kinetic mechanism is illustrated in Scheme 1.

The corresponding steady-state rate equation is given in full by

$$\frac{e}{v} = \frac{1}{k_7} + \frac{1}{k_3} + \frac{k_2 + k_3}{k_1 k_3[\mathrm{A}]} + \frac{k_6 + k_7}{k_5 k_7[\mathrm{B}]} \quad (2)$$

Accordingly the ϕ constants are

$$\phi_0 = \frac{1}{k_7} + \frac{1}{k_3} = \frac{k_3 + k_7}{k_3 k_7} \quad \phi_A = \frac{k_2 + k_3}{k_1 k_3} \quad \phi_B = \frac{k_6 + k_7}{k_5 k_7}$$

In order to further explore the kinetic mechanism, a similar analysis was carried out for two other good substrates, 2-oxohexanoate (Fig. S1, Table S1) and 4,4-dimethyl-2-oxopentanoate (Fig. S2, Table S2). Both gave a similar pattern to that seen above for 2-oxoisocaproate. The resulting kinetic constants are shown in Table 3. The first test that may be applied to these results applies to any ping-pong mechanism: one substrate, glutamate, is kept the same for all the reactions and the constant ϕ_A is given by $(k_2 + k_3)/k_1 k_3$, referring to the rate constants in Scheme 1. Since these only involve the free enzyme E and the complex E-glutamate, it follows that ϕ_A should be the same regardless of the choice of the other substrate. This indeed appears to be borne out, with values of ~ 0.41, 0.38 and 0.44 mM·s for the three substrates used. This constancy contrasts with a more than 20-fold variation in ϕ_B for the same three substrates and provides a further demanding test of the ping-pong mechanism.

The next observation, however, is not a necessary general prediction for a ping-pong mechanism. Inspection of the values of ϕ_0 shows that these also show near-constancy (~ 0.019, 0.018 and 0.017 s). Referring again to Scheme 1, ϕ_0 is given by $1/k_3 + 1/k_7$. If we assume that the value of ϕ_0 is indeed effectively constant for these substrates and that the small differences

Table 2. Kinetic parameters determined by initial-rate measurements of the reaction between 2-oxoisocaproate and glutamate.

	ϕ_0 (s)	$\phi_{2\text{-oxoisocaproate}}$ (mM·s)	$\phi_{glutamate}$ (mM·s)	k_{cat} (s^{-1})	$K_m^{2\text{-oxoisocaproate}}$ (mM)	$K_m^{glutamate}$ (mM)
a	0.0186 ± 0.0013	0.00313 ± 0.0002	0.408 ± 0.0009	53.7 ± 2.13	0.168 ± 0.001	21.9 ± 1.7
b	0.0188 ± 0.0006	0.0032 ± 0.0001	0.407 ± 0.0011	53.2 ± 1.10	0.170 ± 0.001	21.6 ± 0.81
Mean	0.0187	0.0032	0.407	53.5	0.169	21.8

Kinetic data were determined by the use of primary plots against reciprocals of both glutamate concentration (a) and 2-oxoisocaproate concentration (b). Each of these sets of primary plots yields estimates of the three ϕ constants in the initial-rate equation. The alternative methods of plotting yield similar values of the constants and the bottom row in the table shows the mean of the two estimated values.

Table 3. Kinetic constants determined by initial-rate measurements of the reaction between glutamate and two other 2-oxoacid substrates.

Substrate	ϕ_0 (s)	k_{cat} (s^{-1})	$\phi_{glutamate}$ (mM·s)	$K_m^{glutamate}$ (mM)	$\phi_{substrate}$ (mM·s)	$K_m^{substrate}$ (mM)
2-oxoisocaproate	0.0187	53.5	0.407	21.8	0.0032	0.169
4,4-dimethyl-2-oxopentanoate	0.0180	55.8	0.375	20.9	0.085	4.74
2-oxohexanoate	0.0167	59.9	0.441	26.5	0.0449	2.69

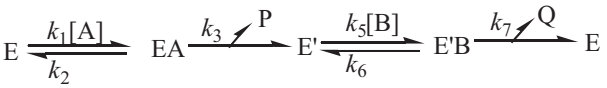

Scheme 1. Reaction scheme for a two-substrate ping-pong mechanism.

merely reflect experimental error, the implication is that $1/k_7$ (unlikely to be constant) must be much smaller than $1/k_3$, in other words that release of 2-oxoglutarate is much slower than release of the product amino acid and is in fact rate-limiting under conditions of substrate saturation. Since both ϕ_A and ϕ_0 appear to be constant for these substrates, their ratio ϕ_A/ϕ_0, which is the true K_m for glutamate at saturating concentration of the other substrate, is necessarily also constant.

Finally we can now return to Table 1 where we noted earlier the striking constancy of the k_{cat} value for all the best substrates. In this case k_{cat} is only an 'apparent' constant since it only applies at the fixed non-saturating concentration of L-glutamate (10 mM) employed in the experiment. However, since by definition the oxoacid concentration is saturating, and therefore eliminates the ϕ_B term in Eqn (1), and since we have seen that the other two ϕ constants in the equation are independent of the nature of the oxoacid, we can now also predict that k_{cat} will be constant with changing oxoacid substrate, not only for 10 mM glutamate but for any arbitrary fixed glutamate concentration. This is a consequence of the deduced inequality $k_7 \gg k_3$. We may assume that for the poorer substrates in Table 1 this inequality no longer applies and that release of product amino acid is largely rate-limiting.

Substrate inhibition

Detailed kinetic analysis of the type described relies on strict adherence to Michaelis–Menten behaviour over an adequate range of substrate concentrations. This was not achievable for all substrates. Even with the substrates shown in Table 3, departure from Michaelis–Menten kinetics was seen over wider ranges of concentration; with 4,4-dimethyl-2-oxopentanoate and 2-oxohexanoate as amino group acceptor, substrate inhibition by glutamate became apparent at 500 mM and 200 mM respectively. Moreover, inhibition by the 2-oxoacid amino acceptor became apparent at much lower concentrations. For instance, in the presence of 10 mM glutamate, increasing the concentration of 4,4-dimethyl-2-oxopentanoate also to 10 mM decreased the rate by 65% compared with the observed maximum (Fig. S3), causing severe departure from linearity in Lineweaver–Burk plots. For three other 2-oxoacids similar inhibition became apparent at lower concentrations, making it impossible to obtain linear plots and good kinetic parameters according to Eqn (1).

In this context, the fact that serious inhibition by glutamate does not supervene until concentrations of at least 200 mM are reached is of considerable practical significance. In application to the synthesis of non-natural amino acids, one of the drawbacks of the aminotransferase reaction is that the equilibrium constant is evenly poised. It is therefore important to be able to drive the reaction forward with high concentrations of glutamate.

Discussion

The broad substrate specificity of the branched-chain aminotransferase of *E. coli* is well established [1,2,5]. The present study, however, has provided quantitative detail with regard to the efficiency of handling a range of both natural and non-natural substrates in the direction of reaction most likely to be of practical application, i.e. the chiral synthesis using L-glutamate as amino donor. This has been possible because of the efficiency of the coupling system employing 2-hydroxyglutarate dehydrogenase to monitor production of 2-oxoglutarate [6]. The previous detailed kinetic study of the enzyme [8] was for the opposite direction of reaction.

Increasingly in the field of biocatalysis, enzymes catalysing a reaction between two or more substrates are analysed by superficial application of a single-substrate approach, in which apparent V_{max} and K_m values are determined only for one fixed concentration of the other substrate(s). The present study emphasizes how

much is to be gained from a more thorough study. Extraction of the full initial-rate equation and the relevant constants has allowed us to give due attention to the striking constancy of the true extrapolated maximum rate for several good substrates and to interpret this in the light of the kinetic mechanism. This in turn makes available critically important information for anyone setting out to improve the catalytic performance of the enzyme. For a currently 'poor' substrate it would be relevant to concentrate on the handling of that oxoacid/amino acid pair by the enzyme; however, for a good substrate improvement can only be achieved by concentrating on the way in which BCAT handles L-glutamate and the product 2-oxoglutarate. In general, the availability of a good coupled assay should make it much easier from now on to assess exactly what has been achieved in any protein engineering experiments with this enzyme.

Materials and methods

Materials

In most cases analytical grade reagents were used. 2-Oxoisocaproate (sodium salt) was purchased from Degussa (Munich, Germany). Other oxoacids and L-amino acids were purchased from Sigma Chemical Co. (St Louis, MO, USA). NADH was obtained from Apollo (Manchester, UK). Fluka (Buchs, Switzerland) supplied PLP. The recombinant *E. coli* BL21(DE3) cells carrying the gene encoding HGDH (EC 1.1.99.2) from *Acidaminococcus fermentans* were a kind gift from W. Buckel (Philipps Universität, Marburg, Germany).

Cloning, expression and purification

A recombinant plasmid containing the *ilv*E gene (Genbank Accession No. NC_000913.2) encoding *E. coli* BCAT was constructed using the expression vector pET23a(+) and transformed into *E. coli* BL21(DE3) cells. The overexpression and purification of BCAT has been described previously [6]. Likewise, HGDH was expressed and purified as detailed in the same paper. This coupling enzyme is now generally available through Enzolve Technologies, Dublin, Ireland.

Coupled assays of BCAT

In the coupled assay for BCAT [6] the activity was measured with a Cary 50 UV–visible spectrophotometer (Agilent Technologies, Cork, Ireland). The assay was conducted at 37 °C in 1 cm light-path cuvettes with 1 mL reaction mixture containing 100 mM Tris/HCl (pH 8.0), 0.13 mM NADH, 10 mM glutamate, 10 mM 2-oxoisocaproate (or other corresponding 2-oxoacids) and coupling enzyme HGDH. The reactions were initiated by the addition of BCAT and the oxidation of NADH was monitored at 340 nm ($\varepsilon = 6220\ M^{-1}\cdot cm^{-1}$).

In the standard assays, stock solutions of the coupling enzymes kept in a −20 °C freezer were thawed, diluted with 100 mM Tris/HCl (pH 8.0) containing 2 $mg\cdot mL^{-1}$ bovine serum albumin and stored on ice. The activity measurement of HGDH was carried out spectrophotometrically at 37 °C by monitoring the decrease of A_{340} caused by oxidation of NADH. The activity was determined in 100 mM Tris/HCl buffer (pH 8.0) containing 0.13 mM NADH and 10 mM 2-oxoglutarate with a final volume of 1 mL. At least three replicate readings were performed for each assay and averaged. The range of the three readings was never more than 5% and for the majority of readings was within 2%.

Unless otherwise stated, reactions were started by the addition of purified BCAT, which was diluted from stock solutions (containing 50% glycerol) with 100 mM Tris/HCl (pH 8.0) containing 2 $mg\cdot mL^{-1}$ bovine serum albumin. All substrates and NADH solutions were freshly prepared. Reaction solutions were adjusted to pH 8.0 ± 0.05 with NaOH or HCl, and incubated at 37 °C during the measurements. An appropriate activity range of added coupling enzyme [6] is 80–130 U. When an excess amount of HGDH was thus used, after a short initial lag phase the reaction traces were linear and the steady-state rates of the coupled assays were found to be directly proportional to the concentrations of BCAT.

Initial-rate kinetic analysis of BCAT

First, apparent kinetic constants of BCAT at a fixed concentration of glutamate were determined for nine 2-oxoacid substrates by measuring rates of transamination in 1 mL reaction mixtures containing 100 mM Tris/HCl (pH 8.0), 0.13 mM NADH, 10 mM glutamate, purified BCAT and coupling enzyme (HGDH) plus 2-oxoacid at concentrations varying from 0.01 mM to 10 mM. The reactions were initiated by addition of 10 μL 2-oxoacids. The whole set of bi-bi kinetic studies was carried out three times with each substrate in order to optimize experimental design. In each case the results reported are for the third optimized experiment. Apparent K_m and V_{max} values were calculated by fitting the Michaelis–Menten equation to the experimental data using the non-linear least-squares fit mode of PRISM 4 (GraphPad Software, San Diego, CA, USA).

Acknowledgements

We are grateful to Professor Wolfgang Buckel (Philipps Universität, Marburg, Germany) for his kind gift

of recombinant *E. coli* cells carrying the gene encoding (*R*)-2-hydroxyglutarate dehydrogenase from *A. fermentans*. Financial support from Wuhan Science and Technology Bureau (to X.-G.W.) and Enterprise Ireland, the Royal Irish Academy and the Science Foundation Ireland (to P.C.E.) is gratefully acknowledged. X.Y. was supported by a postgraduate scholarship under the EMBARK scheme of the Irish Research Council for Science, Engineering and Technology and also by the Chinese Scholar Scheme operating between University College Dublin and the Chinese Scholar Council.

References

1 Taylor PP, Pantaleone DP, Senkpeil RF & Fotheringham IG (1998) Novel biosynthetic approaches to the production of unnatural amino acids using transaminases. *Trends Biotech* **16**, 412–418.
2 Hwang B-Y, Cho B-K, Yun H, Koteshwar K & Kim B-G (2005) Revisit of aminotransferase in the genomic era and its application to biocatalysis. *J Mol Catal B Enz* **37**, 47–55.
3 Faber K & Kroutil W (2005) New enzymes for biotransformations. *Curr Opin Chem Biol* **9**, 181–187.
4 Rudat J, Brucher BR & Syldatk C (2012) Transaminases for the synthesis of enantiopure beta-amino acids. *AMB Express* **2**, 1–10.
5 Hong E, Cha M, Yun H & Kim B-G (2010) Asymmetric synthesis of L-*tert*-leucine and L-3-hydroxyadamantylglycine using branched chain aminotransferase. *J Mol Catal B Enz* **66**, 228–233.
6 Yu X, Bresser J, Schall I, Djurdjevic I, Buckel W, Wang X & Engel PC (2012) Development of a satisfactory and general continuous assay for aminotransferases by coupling with (*R*)-2-hydroxyglutarate dehydrogenase. *Anal Biochem* **431**, 127–131.
7 Lee-Peng FC, Hermodson MA & Kohlhaw GB (1979) Transaminase B from *Escherichia coli*: quaternary structure, amino-terminal sequence, substrate specificity, and absence of a separate valine-alpha-ketoglutarate activity. *J Bact* **139**, 339–345.
8 Inoue K, Kuramitsu S, Aki K, Watanabe Y, Takagi T, Nishigai M, Ikai A & Kagamiyama H (1988) Branched-chain amino acid aminotransferase of *Escherichia coli*: overproduction and properties. *J Biochem* **104**, 777–784.
9 Velick SF & Vavra J (1962) A kinetic and equilibrium analysis of the glutamate oxaloacetate transaminase mechanism. *J Biol Chem* **237**, 2109–2122.
10 Al-Haque N, Santacoloma PA, Neto W, Tufvesson P, Gani R & Woodley JM (2012) A robust methodology for kinetic model parameter estimation for biocatalytic reactions. *Biotech Progr* **28**, 1186–1196.
11 Seo YM & Yun H (2011) Enzymatic synthesis of L-*tert*-leucine with branched chain aminotransferase. *J Microbiol Biotech* **21**, 1049–1052.
12 Li T, Kootstra AB & Fotheringham IG (2002) Nonproteinogenic alpha-amino acid preparation using equilibrium shifted transamination. *Org Process Res Dev* **6**, 533–538.
13 Then JBK, Deger H, Grabley S & Marquardt R (1987) Verfahren zur Herstellung von L-tertiär-Leucin durch Transaminierung. EP Patent Number 0,533,216 A531.
14 Wang X-G, Zhang P, Lynch S & Engel PC (2010) Forced evolution of *Escherichia coli* cells with the ability to effectively utilize non-natural amino acids L-*tert*-leucine, L-norleucine and γ-methyl-L-leucine. *Biocat Biotrans* **28**, 293–303.
15 Xian M, Alaux S, Sagot E & Gefflaut T (2007) Chemoenzymatic synthesis of glutamic acid analogues: substrate specificity and synthetic applications of branched chain aminotransferase from *Escherichia coli*. *J Org Chem* **72**, 7560–7566.
16 Bommarius AS, Schwarm M & Drauz K (1998) Biocatalysis to amino acid-based chiral pharmaceuticals – examples and perspectives. *J Mol Catal B Enz* **5**, 1–1.
17 Krix G, Bommarius AS, Drauz K, Kottenhahn M, Schwarm M & Kula MR (1997) Enzymatic reduction of alpha-keto acids leading to L-amino acids, D- or L-hydroxy acids. *J Biotech* **53**, 29–39.
18 Hans UB, Peter S & August WW (1978) Optimization of methods for aspartate aminotransferase and alanine aminotransferase. *Clin Chem* **24**, 58–73.
19 Carl PH & Cleland WW (1964) Kinetic studies of glutamic oxaloacetic transaminase isozymes. *Biochemistry* **3**, 338–345.
20 Okada K, Hirotsu K, Hayashi H & Kagamiyama H (2001) Structures of *Escherichia coli* branched-chain amino acid aminotransferase and its complexes with 4-methylvalerate and 2-methylleucine: induced fit and substrate recognition of the enzyme. *Biochemistry* **40**, 7453–7463.
21 Goto M, Miyahara I, Hayashi H, Kagamiyama H & Hirotsu K (2003) Crystal structures of branched-chain amino acid aminotransferase complexed with glutamate and glutarate: true reaction intermediate and double substrate recognition of the enzyme. *Biochemistry* **42**, 3725–3733.
22 Dalziel K (1957) Initial steady state velocities in the evaluation of enzyme–coenzyme–substrate reaction mechanisms. *Acta Chem Scand* **11**, 1706–1723.
23 Engel PC (1981) Enzyme Kinetics: the Steady-State Approach, 2nd edn. Chapman and Hall, London.

Supporting information

Additional supporting information may be found in the online version of this article at the publisher's web site:

Fig. S1. Double reciprocal plot of reaction rates for variable fixed concentrations of 2-oxohexanoate at various fixed concentrations of L-glutamate.

Fig. S2. Double reciprocal plot of reaction rates for variable fixed concentrations of 4,4-dimethyl-2-oxopentanoate at various fixed concentrations of L-glutamate.

Fig. S3. Substrate inhibition curve of 4,4-dimethyl-2-oxopentanoate in the BCAT catalysed transamination reaction in the presence of 10 mM L-glutamate.

Table S1. Kinetic parameters determined by initial-rate measurements for substrates 2-oxohexanoate and glutamate.

Table S2. Kinetic parameters determined by initial-rate measurements for substrates 4,4-dimethyl-2-oxopentanoate and glutamate.